Pion inelastic scattering to the low-lying excited states of ^{6}Li

R. R. Kiziah,* M. D. Brown,† C. J. Harvey,‡ D. S. Oakley,
D. P. Saunders,* P. A. Seidl, and C. F. Moore
University of Texas at Austin, Austin, Texas 78712

W. B. Cottingame,§ R. W. Garnett, Steven J. Greene,§
G. A. Luna,** and G. R. Burleson
New Mexico State University, Las Cruces, New Mexico 88003

D. B. Holtkamp§
University of Minnesota, Minneapolis, Minnesota 55455
(Received 2 August 1984)

The excitation function for π^+ inelastic scattering to the 0^+, $T=1$, 3.563-MeV level of ^{6}Li has been measured at a constant momentum transfer $q\simeq 109$ MeV/c for incident pion energies from 100 to 260 MeV. Although the differential cross sections extracted for the natural-parity transitions to the 3^+, $T=0$, 2.185-MeV and 2^+, $T=0$, 4.25-MeV levels are well reproduced within the framework of the distorted-wave impulse approximation, distorted-wave impulse approximation calculations fail to reproduce the anomalous excitation function observed for the transition to the 3.563-MeV level. The shape of the 3.563-MeV excitation function is similar to that previously observed for $\pi^\pm$ inelastic scattering to the 1^+, $T=1$, 15.11-MeV state of ^{12}C [C. L. Morris *et al.*, Phys. Lett. **108B**, 172 (1982)]. The same mechanism may be responsible for the observed excitation functions of both $\Delta S=\Delta T=1$ transitions. A possible mechanism is the previously proposed direct excitation of Δ-particle–nucleon-hole (Δ-h) components in the wave functions.

I. INTRODUCTION

Comparison of pion-inelastic-scattering data in the energy range of the (3,3) resonance with calculations using the distorted-wave impulse approximation (DWIA) and well-known transition densities, indicates that a single-step, impulse approximation is an adequate description for pion-induced transitions to nuclear states which are strongly excited. For example, Lee and Kurath[1] and Lee and Lawson,[2] using the DWIA and transition densities derived from shell-model wave functions, qualitatively reproduce angular distributions for pion inelastic scattering to excited states of various p- and sd-shell nuclei. Morris *et al.*[3] and Boyer *et al.*[4] obtain good agreement between angular distributions and DWIA calculations, which use empirical transition densities determined from electron-scattering data, for inelastic scattering to low-lying collective states in ^{12}C, ^{40}Ca, ^{42}Ca, ^{44}Ca, and ^{48}Ca. Furthermore, the excitation functions measured at a constant momentum transfer for the unnatural-parity transitions to the 4^-, 19.25-MeV state and 2^- structure at approximately 18.4 MeV in ^{12}C (Ref. 5) and the $\frac{9}{2}^+$, 9.5-MeV state in ^{13}C (Ref. 6) decrease with increasing incident pion energy as predicted by the DWIA.[7] Within the framework of the DWIA, these unnatural-parity transitions are particularly simple, involving only the spin-dependent part of the effective pion-nucleus inelastic interaction and the transverse spin transition density.[8] In particular, for the unnatural-parity transitions to states of stretched configuration in ^{16}O (4^- levels at $E_x=17.79$, 18.98, and 19.80 MeV) and ^{28}Si (6^- levels at $E_x=11.58$ and 14.36 MeV), Carr *et al.*[9] satisfactorily reproduce the measured angular distributions with DWIA calculations using spin transition densities fixed from (e,e′) and (p,p′) data.

For pion-induced excitation of nuclear states that are weakly excited by a one-step, impulse-approximation mechanism, nuclear medium effects and multistep processes may be important and there may not be good agreement between the pion-inelastic-scattering data and DWIA calculations, as for the above strongly excited examples. This is indeed the case for the $T=1$ member of the weakly excited 1^+ doublet, 12.71 MeV ($T=0$) and 15.11 MeV ($T=1$), of ^{12}C.[10] Cohen-Kurath wave functions[11] describe the 15.11- and 12.71-MeV states as near analogs, and this description for the spin transition densities is supported by (e,e′) data.[12] Calculations using a one-step, DWIA mechanism predict the ratio of cross sections for unnatural-parity transitions to members of an antianalog-analog pair to be four to one.[8,10] Both the constant-momentum-transfer-excitation function and the angular distributions for the 12.71-MeV state are well reproduced by DWIA calculations. However, the measured ratio of four times the averaged π^+ and π^- differential cross sections for the 15.11-MeV state to the averaged π^+ and π^- differential cross sections for the 12.71-MeV state deviates significantly from one, especially at energies near 180 MeV (ratio is approximately three), and displays a rapidly varying energy dependence. (Averaging the π^+ and π^- differential cross sections removes the effect of isospin mixing between the two states on the ratio to better than 1%.[10]) Also, DWIA calcula-

tions do not agree with the 15.11-MeV angular distributions at energies near the (3,3) resonance.[12]

Uncertainties in the spin transition density or inadequacies in the spin-dependent piece of the effective pion-nucleus interaction are an unlikely explanation[10] for the anomalous excitation function for the $\Delta S=\Delta T=1$ transition to the 15.11-MeV level of ^{12}C. Rather, a more likely explanation is that an additional process other than a one-step, impulse-approximation mechanism is contributing to the isovector transition. Therefore, to further investigate pion-induced excitation of weakly excited nuclear levels, we consider the $\Delta S=\Delta T=1$ transition from the 1^+, $T=0$, ground state of ^{6}Li to the 0^+, $T=1$, 3.563-MeV level. We have measured an excitation function for π^+ inelastic scattering to the 3.563-MeV state of ^{6}Li at incident pion energies from 100 to 260 MeV and partial angular distributions at 120 and 180 MeV. We also present in Table I the differential cross sections for elastic scattering and for inelastic scattering to the 2.185- and 4.25-MeV states. The 2.185- and 4.25-MeV differential cross sections are compared to microscopic DWIA calculations using transition densities derived from Cohen-Kurath wave functions.[11] The 3.563-MeV differential cross sections are compared to microscopic DWIA calculations using spin transition densities derived from Cohen-Kurath wave functions,[11] the empirical shell-model wave functions of Donnelly and Walecka,[13] and the phenomenological wave functions of Bergstrom *et al.*[14]

II. DATA ACQUISITION AND REDUCTION

The data were collected using the energetic pion channel and spectrometer (EPICS) system[15] at the Clinton P. Anderson Meson Physics Facility (LAMPF). Four separate targets consisting of sheets of enriched lithium, $\geq 98\%$ ^{6}Li, fabricated by the Oak Ridge National Laboratory were used during the experiment. Two of the targets, with dimensions of 22.9 cm $\times$ 15.2 cm and areal densities of 202 and 100 mg/cm^2, were used for approximately one-half of the total data acquisition and contained no discernible contamination. The remaining two targets, with dimensions of 20 cm $\times$ 10 cm and areal densities of 205 and 95 mg/cm^2, were contaminated by exposure to the air during shipping. Hydrogen contamination was

TABLE I. Differential cross sections for π^+ elastic scattering and inelastic scattering to the 3^+, 2.185-MeV; 0^+, 3.563-MeV; and 2^+, 4.25-MeV levels of ^{6}Li.

T_π (MeV)	$\theta_{c.m.}$ (deg)	q[a] (fm^{-1})	Elastic $d\sigma/d\Omega_{c.m.}$ (mb/sr)	3^+, 2.185 MeV $d\sigma/d\Omega_{c.m.}$ (mb/sr)	0^+, 3.563 MeV $d\sigma/d\Omega_{c.m.}$ (μb/sr)	2^+, 4.25 MeV $d\sigma/d\Omega_{c.m.}$ (mb/sr)
100	34.3	0.55	27.2±0.1	0.397±0.017	39.8±2.2	0.147±0.005
120	15.7	0.29	80.5±0.4	0.271±0.003	33.9±3.0	0.079±0.005
120	21.9	0.40	74.1±0.4	0.307±0.042	43.6±4.6	0.091±0.008
120	25.1	0.46	64.0±0.3	0.569±0.032	61.5±5.6	0.137±0.009
120	28.2	0.51	49.1±0.2	0.632±0.033	41.3±4.7	0.259±0.014
120	28.2	0.51	48.8±0.2	0.587±0.030	48.4±4.1	0.203±0.008
120	30.3	0.55	43.0±0.3	0.737±0.040	57.0±4.3	0.276±0.009
120	33.4	0.61	34.9±0.2	0.799±0.030		
120	33.4	0.61	35.1±0.2	0.853±0.037	38.0±3.3	0.274±0.007
120	38.6	0.69			32.8±3.2	0.395±0.007
120	43.7	0.79	15.0±0.1	0.973±0.029	22.3±3.2	0.335±0.007
120	48.9	0.87	8.2±0.1	0.975±0.028	12.3±2.3	0.274±0.005
140	27.2	0.55	64.9±0.3	1.11 ±0.05	60.7±4.4	0.315±0.009
160	25.2	0.55	80.5±0.3	1.36 ±0.06	68.5±5.5	0.505±0.011
170	24.7	0.57			70.2±7.0	0.607±0.011
170	24.7	0.57	85.4±0.5	1.78 ±0.09	80.7±9.4	0.637±0.021
180	21.1	0.50	103.4±0.4	1.25 ±0.07	117.0±7.6	0.855±0.018
180	24.3	0.58	79.4±0.3	1.74 ±0.06	100.0±7.7	0.690±0.015
180	24.3	0.58	79.5±0.5	1.62 ±0.08	95.0±9.4	0.801±0.021
180	24.3	0.58	79.3±0.4	1.59 ±0.06		
180	24.3	0.58	80.9±0.5	1.68 ±0.09	62.0±9.1	0.763±0.019
180	27.4	0.65	61.3±0.3	1.97 ±0.06	55.0±5.6	0.829±0.012
180	30.6	0.72	44.7±0.2	2.32 ±0.06	43.1±6.3	0.883±0.014
190	23.2	0.57			97.0±12.0	0.870±0.030
190	23.2	0.57			89.5±9.5	0.981±0.030
200	21.7	0.56			81.7±6.4	0.607±0.013
200	21.7	0.56	100.7±0.7	1.96 ±0.12	97.0±5.7	0.737±0.012
215	20.7	0.56	107.0±0.5	1.88 ±0.09	73.3±5.6	0.892±0.012
230	19.7	0.55	105.7±0.7	2.03 ±0.12	55.9±7.3	0.707±0.015
230	19.7	0.55	103.4±1.5	2.09 ±0.25	55.6±6.0	0.703±0.013
260	18.2	0.56	109.8±0.8	2.06 ±0.13	33.1±10.5	0.713±0.021

[a]The q values were calculated for an excitation energy of 2.185 MeV.

negligible in the thick 20 cm $\times$10 cm target ($\leq$1%) but appreciable in the thin 20 cm$\times$10 cm target ($\simeq$5%). Since we clearly observed the 6.13- and 6.92-MeV states of ^{16}O in some π^+ Q-value spectra but never observed any inelastic peaks of ^{14}N (Ref. 16), we assumed the heavy impurity to be ^{16}O. With this assumption, the total amounts of impurities for the thick and thin 20 cm $\times$10 cm targets were 2.3% and 18%, respectively. A comparison of differential cross sections for the elastic scattering from ^{6}Li, extracted from the contaminated and uncontaminated targets at the same incident pion energy and scattering angle, indicate that the estimated amounts of impurities are accurate within $\leq$1%. ^{7}Li was not detected in any of the targets.

Figure 1 shows the Q-value spectrum for ^{6}Li($\pi^+,\pi^{+\prime}$) using the 205 mg/cm^2, 20 cm $\times$10 cm target for T_π=140 MeV and θ_{lab}=26°. This spectrum is representative of the spectra used for determination of cross sections for excitation of the 3.563- and 4.25-MeV levels. Although the experimental resolution was not the best for the 205 mg/cm^2 target [240 keV full width at half maximum (FWHM)], the 3.563-MeV level is clearly resolved from the large continuum background and the 4.25-MeV level. The discontinuity in the Q-value spectrum between the ground state and 2.185-MeV state is an artifact of the hardware veto of elastic counts used to limit data rates during data acquisition by rejecting the majority of events with a Q value below $\simeq$1.2 MeV. The elastic and 2.185-MeV cross sections were determined without the use of this hardware veto (see the insert in Fig. 1).

Peak areas were extracted from the Q-value spectra using the computer program LOAF.[17] The backgrounds under the elastic and 3^+ peaks were fitted with a first-order polynomial, while the backgrounds under the 0^+ and 2^+ peaks were fitted with a third-order polynomial. Line shapes for the elastic and 3^+ peaks were extracted from the spectra for each target at each incident pion energy because the resolution varied with energy from 200 keV (220 keV) FWHM at T_π=100 MeV to 260 keV (260 keV) FWHM at T_π=260 MeV for the thin (thick) targets. The line shape of the 0^+ peak was taken to be the same as the 3^+, while the line shape of the 2^+ was constructed by folding the line shape used for the 3^+ with a Lorentzian of 680 keV FWHM. The peak positions were constrained to be 0.0, 2.185 (Ref. 18), 3.563 (Ref. 18), and 4.25 MeV. Both the position and natural width of the 2^+ level, 4.25$\pm$0.02 MeV and 680$\pm$20 keV, were determined from fits to several spectra where this state was predominant. Previous determinations from other experiments are 4.27$\pm$0.04 MeV and 690$\pm$120 keV,[19] 4.29$\pm$0.02 MeV and 850$\pm$50 keV,[20] and 4.30$\pm$0.01 MeV and 480$\pm$80 keV.[20] The 5.37- and 5.65-MeV states were not observed in the spectra, and thus no attempt was made to include them in the fits.

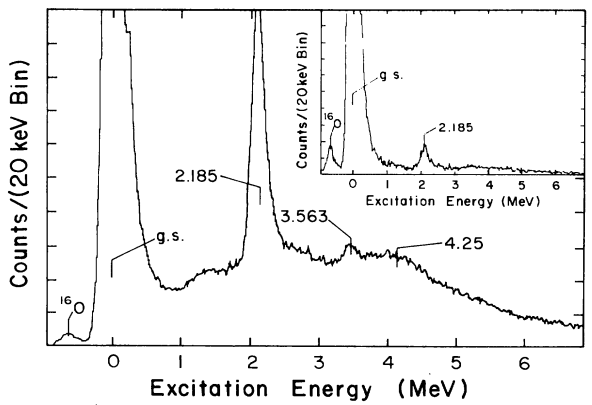

FIG. 1. A typical π^+ energy-loss spectrum taken at T_π=140 MeV and θ_{lab}=26° for which the hardware veto of elastic events was used. The insert is the π^+ energy-loss spectrum without the use of the hardware veto.

The consistency of the fits to the various Q-value spectra was checked by extracting areas for 100 keV wide segments of background centered about 3.563 and 4.25 MeV. Plots of the background yields for both the 3.563- and 4.25-MeV segments resulted in smooth and continuous angular distributions at 120 and 180 MeV. Also the background yields versus incident pion energy are smooth and continually increasing. We therefore have indication that our extraction of the peak areas from the large continuum background is consistent at different incident pion energies and scattering angles.

Experimental yields were measured for $\theta_{lab}\geq$25° by monitoring the EPICS channel beam flux with an ionization chamber located downstream from the scattering target. For $\theta_{lab}<$25° the ionization chamber was not used since it partially blocked the spectrometer entrance. For these angles, relative normalization was accomplished through an ionization chamber located within the pion production target cell and a charge integrating toroidal coil located upstream of the pion production target. Monitoring of the ratio of the ionization chamber current to the currents from these two monitors of the proton beam showed $\leq$2% fluctuations for $\theta_{lab}\geq$25°, establishing them as reliable beam flux monitors. Absolute cross sections were calculated by normalizing to π^+ scattering on hydrogen (CH_2 targets of dimensions 22.9 cm$\times$15.2 cm and 20 cm$\times$10 cm corresponding to the two different sizes of ^{6}Li targets) using Coulomb-corrected phase-shift predictions from the computer code CROSS (Ref. 21) with the phase shifts of Rowe, Salomon, and Landau.[22]

The data were corrected for computer live time, multiwire proportional drift chamber efficiency, pion survival fraction through the spectrometer, and the variation of the spectrometer's solid angle with pion momentum. The quoted error bars are statistical only. Total systematic errors are estimated to be $\simeq\pm$7% due to uncertainties of $\pm$3% in chamber efficiency, $\pm$3% in pion survival fraction, $\pm$2% in the spectrometer's solid angle variation with momentum in the spectrometer, $\pm$3% in channel beam monitoring, and $\pm$3% in normalization to π^+ scattering on hydrogen. Furthermore, the data for the 3.563- and 4.25-MeV states contain additional systematic errors of $\pm$15% and $\pm$10%, respectively, due to the uncertainty in the fitting of the large continuum background and the uncertainty in the position and width of the 2^+ state. These systematic errors were inferred by varying the order of the polynomial fit to the background, and by

varying the position and width of the 2^+ state from 4.23 to 4.27 MeV and 660 to 700 keV.

III. DATA ANALYSIS

A. Elastic scattering analysis

The first-order, zero-range, impulse-approximation elastic calculations were performed with a variation[23] of the coordinate-space computer program PIRK,[24] which solves a Klein-Gordon equation, using only linear terms in the optical-model potential. For all ^{6}Li elastic calculations, we used the Kisslinger form[25] of the optical-model potential given by

$$V(r) = -Ak_\pi^{-2} b_0 \rho(r) + Ab_1 \vec{\nabla}\rho(r)\cdot\vec{\nabla} , \quad (1)$$

where $\rho(r)$ is the nucleon density normalized to unity, k_π is the laboratory momentum of the incident pion, and A is the mass of the target. The complex b_0 and b_1 coefficients are constructed from the pion-nucleon phase shifts of Rowe, Salomon, and Landau[22] evaluated at an energy of 30.0 MeV below the incident pion beam energy. This procedure has been demonstrated by Cottingame and Holtkamp[23] to give better agreement to pion-elastic-scattering data for nuclei ranging from ^{9}Be to ^{208}Pb. This phenomenological shift in the collision energy is a method for adjusting the pion-nucleus kinematics so as optimally to factorize the optical-model potential (see Ref. 12 for a discussion of the above procedure). The proton matter density distribution was characterized by a three-parameter phenomenological distribution taken from elastic electron scattering[26] with the finite size of the proton charge removed. This distribution has the form

$$\rho(r) = Z/(8\pi^{3/2})\{(1/a^3)\exp(-r^2/4a^2) - [c^2(6b^2-r^2)/4b^7] \times \exp(-r^2/4b^2)\} , \quad (2)$$

with $a=0.928$ fm, $b=1.26$ fm, and $c=0.48$ fm.[26] This phenomenological distribution was also used for the neutron matter density distribution.

The present 120- and 180-MeV π^+ elastic data, the Swiss Institute for Nuclear Research (SIN) 164-MeV π^- elastic data,[27] and elastic calculations are presented in Fig. 2. Since the elastic optical potential is used for the generation of the distorted waves for inelastic calculations, the good agreement indicates adequate handling of the distortions.

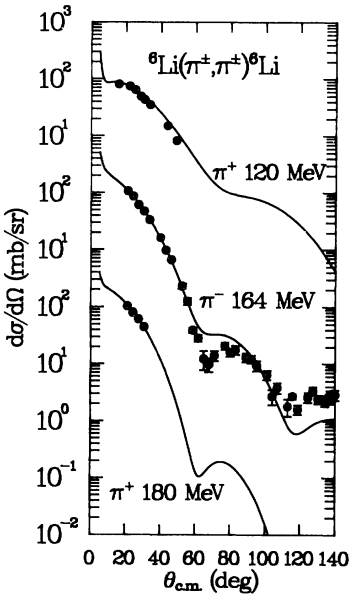

FIG. 2. Differential cross sections for π^+ and π^- elastic scattering for ^{6}Li for $T_\pi = 120$, 164, and 180 MeV. The calculations include a -30 MeV shift in the energy at which the optical model parameters are calculated. The 164-MeV data are from Ref. 27.

B. Inelastic scattering analysis

The inelastic calculations presented in this paper are Born approximation, DWIA calculations in which the pion-nucleus transition amplitude is a configuration-space, folded product of a distortion function and form factor. The distortion function, a product of initial and final pion distorted waves, is computed from the elastic optical-model potential employed in the elastic calculations. Calculation of the form factor, whose specific form depends upon the inelastic transition and is the folded product of the pion-nucleon interaction and the nuclear transition density, uses the frozen-target approximation assuming on-shell kinematics and a collision energy obtained from the elastic calculations. For inelastic calculations using Cohen-Kurath wave functions,[11] we use a modification of the generalized inelastic scattering potential code ALLWRLD (Ref. 28) to calculate the form factor. The harmonic oscillator parameters and renormalization constants include the standard center-of-mass correction needed when using shell-model wave functions. The distortion function and differential cross sections are then generated from the code UTDWPI.[29] For all other inelastic calculations we use only the code UTDWPI and no center-of-mass correction is included in the harmonic oscillator parameters and renormalization constants. However, these inelastic calculations use center-of-mass corrected form factors with the correction being applied in momentum space.

1. 3^+, $T=0$, 2.185-MeV state

Electron-scattering data indicate that the natural-parity transition to the 2.185-MeV level of ^{6}Li is almost completely longitudinal, with measurements in the region of $q=0.7-1.8$ fm^{-1} yielding a transverse form factor which is less than 2% of the longitudinal form factor.[30] Since the spin-orbit transition density is approximately zero, the form factor involves only the central component of the pion-nucleon interaction and the isoscalar matter transition density.[31] Inelastic calculations for this natural-parity transition have been performed using two different transition densities derived from pure LS-coupling and Cohen-Kurath intermediate-coupling p-shell wave functions. Each calculation employed equal transition densi-

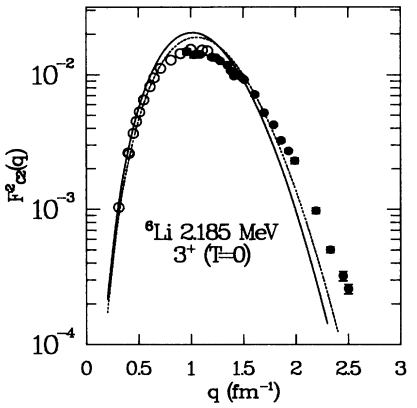

FIG. 3. $F_L^2(q)$ for the 3^+, $T=0$, 2.185-MeV state of ^{6}Li. The calculations used microscopic transition densities derived from pure LS-coupling (solid curve) and Cohen-Kurath intermediate-coupling (dashed curve) p-shell wave functions with $\alpha=0.534$ fm^{-1} and a renormalization constant of 2.03 and $\alpha=0.558$ fm^{-1} and a renormalization constant of 1.93, respectively. The data are from Refs. 14 (solid circles) and 34 (open circles).

ties for the protons and neutrons. The harmonic oscillator parameter, α, and renormalization constant for the transition density derived from the pure LS-coupling p-shell wave functions are 0.534 fm^{-1} and 2.03. These values were required to fit the inelastic-electron-scattering data considered in Ref. 32 and give good agreement between theory and experiment for the ^{6}Li(p,p')^{6}Li*(2.185 MeV) differential cross sections at $E_p \simeq 25$ and 45 MeV.[32] The transition density derived from the intermediate-coupling p-shell wave functions uses $\alpha=0.558$ fm^{-1} and a renormalization constant of 1.93, again determined from (e,e') data.[33] Electron-scattering longitudinal form factors from Refs. 14 and 34 are shown in Fig. 3. The solid (dashed) curves correspond to the transition densities computed from the pure LS- (intermediate-) coupling p-shell wave functions. Both theoretical form factors are similar, with the intermediate-coupling form factor in better agreement with the electron-scattering data. The π^+ 2.185-MeV data and calculations for $T_\pi=120$ and 180 MeV are presented in Fig. 4. Figure 5 shows the data and calculations for $T_\pi=100$–260 MeV with the differential cross sections corresponding to a constant momentum transfer $q \simeq 109$ MeV/c. From the data and calculations, the first maxima of the angular distributions for the 2.185-MeV state are expected to be at $q \simeq 164$ MeV/c. The intermediate-coupling calculation is in good agreement with both the 120- and the 180-MeV experimental angular distributions. Furthermore, this calculation reproduces well the constant-q experimental differential cross sections, considering that the theoretical values plotted in Fig. 5 are taken from the steep forward slope of the various angular distributions where errors would produce the greatest variations. The pure LS-coupling calculation yields similar shapes for the 120- and 180-MeV angular distributions and the constant-q differential cross sections as does the intermediate-coupling calculation but overestimates the magnitudes. Such disagreement suggests that the renormalization constant is too large.

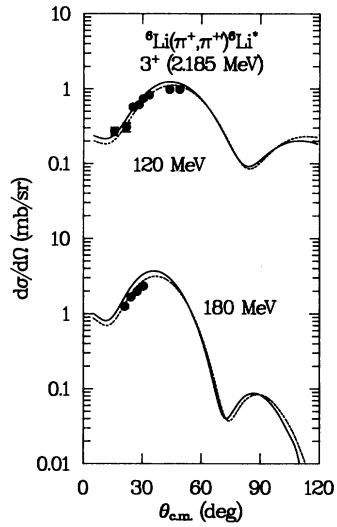

FIG. 4. Angular distributions for π^+ inelastic scattering to the 3^+, $T=0$, 2.185-MeV state of ^{6}Li for $T_\pi=120$ and 180 MeV. The calculations used microscopic transition densities derived from pure LS-coupling (solid curve) and Cohen-Kurath intermediate-coupling (dashed curve) p-shell wave functions with $\alpha=0.534$ fm^{-1} and a renormalization constant of 2.03 and $\alpha=0.558$ fm^{-1} and a renormalization constant of 1.93, respectively.

2. 2^+, $T=0$, 4.25-MeV state

The electron-scattering form factors for both natural-parity transitions to the 2.185- and 4.25-MeV levels have the same dependences on the momentum transfer.[35] Therefore, the transition to the 4.25-MeV state is principally longitudinal, and we treat this transition as com-

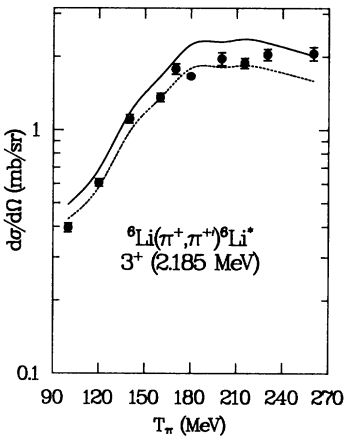

FIG. 5. Differential cross sections for π^+ inelastic scattering to the 3^+, $T=0$, 2.185-MeV state of ^{6}Li at a constant $q \simeq 109$ MeV/c. The calculations used microscopic transition densities derived from pure LS-coupling (solid curve) and Cohen-Kurath intermediate-coupling (dashed curve) p-shell wave functions with $\alpha=0.534$ fm^{-1} and a renormalization constant of 2.03 and $\alpha=0.558$ fm^{-1} and a renormalization constant of 1.93, respectively.

pletely analogous to the excitation of the 2.185-MeV level. However, even though the 4.25-MeV state is observed in (e,e′) spectra, a detailed form factor has not been measured because of this state's large natural width, the overlapping 5.37-MeV state, and the large continuum background.[36] We therefore cannot deduce a transition density from electron-scattering data as was the case for the 2.185-MeV transition. Thus, we simply used a transition density derived from Cohen-Kurath intermediate-coupling p-shell wave functions with $\alpha=0.52$ fm^{-1} and a renormalization constant of 0.82 determined from fitting only our $(\pi^+,\pi^{+\prime})$ data at $T_\pi=120$ and 180 MeV. This transition density yields a radiative width, $\Gamma_{\gamma 0}^{(E2)}$, of 3.02 eV in agreement with the experimental value of 5.4 ± 2.8 eV.[19] The 4.25-MeV experimental and theoretical 120- and 180-MeV angular distributions and the constant-q differential cross sections are shown in Figs. 6 and 7, respectively. The agreement is not as good as for the 2.185-MeV state but is very reasonable considering the difficulties in extracting the cross sections and possible uncertainties in the transition density.

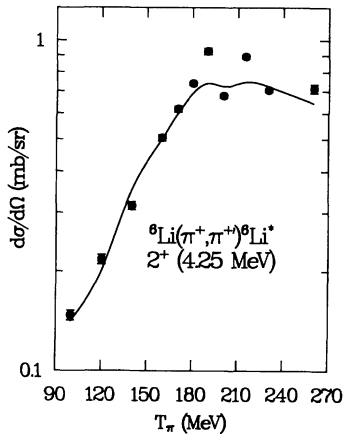

FIG. 7. Differential cross sections for π^+ inelastic scattering to the 2^+, $T=0$, 4.25-MeV state of ^{6}Li at $q\simeq109$ MeV/c. The calculation used a microscopic transition density derived from Cohen-Kurath intermediate-coupling p-shell wave functions with $\alpha=0.52$ fm^{-1} and a renormalization constant of 0.82.

3. 0^+, $T=1$, 3.563-MeV state

As is the case for the natural-parity transitions to the 2.185- and 4.25-MeV levels of ^{6}Li, the Born approximation, DWIA description of the pion-induced unnatural-parity transition to the 3.563-MeV state is straightforward, involving only a single component of the pion-nucleon interaction and a single nuclear transition density. Using a single scattering model, the spin-dependent piece of the interaction is represented by the zero-range spin-orbit operator,[9] and the transition density is the transverse spin transition density. We employed three different transverse spin transition densities determined from fits to various (e,e′) measurements but compared to the most recent sets of (e,e′) data (Refs. 14 and 37). The proton and neutron transition densities were taken to be equal. The reasons for using three transition densities are the following: (1) The p-shell harmonic oscillator basis is known to result in a poor description of the 3.563-MeV electron-scattering transverse form factor over the entire second lobe, $q>1.4$ fm^{-1}. We therefore employ one transition density which reproduces both the first and second lobes of the form factor. (2) Since there is no analog to the 3.563-MeV state as is the situation for the 12.71-/15.11-MeV antianalog-analog pair of ^{12}C, any anomalies in the 3.563-MeV excitation function depend upon comparison of theory with data and not data for analogs as for the 15.11-MeV level. Thus, accurate spin transition densities are imperative.

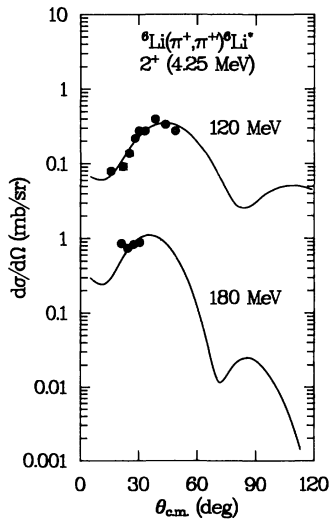

FIG. 6. Angular distributions for π^+ inelastic scattering to the 2^+, $T=0$, 4.25-MeV state of ^{6}Li for $T_\pi=120$ and 180 MeV. The calculation used a microscopic transition density derived from Cohen-Kurath intermediate-coupling p-shell wave functions with $\alpha=0.52$ fm^{-1} and a renormalization constant of 0.82.

The first analysis for the spin-flip transition to the 3.563-MeV state used a spin transition density derived from Cohen-Kurath intermediate-coupling p-shell wave functions. The harmonic oscillator parameter was chosen to be 0.518 fm^{-1} from the work of Petrovich *et al.*,[32] who fitted low q electron-scattering data using pure LS-coupling p-shell wave functions. We used a renormalization constant of 0.97. Petrovich *et al.* conclude that both sets of theoretical wave functions provide an adequate description of the experimental static moments and transition probabilities of ^{6}Li with the exception of the quadrupole moment.[32] However, we chose the intermediate-coupling p-shell wave functions because they give a slightly better fit to the most recent sets of (e,e′) data (Refs. 14 and 37) for the inelastic $M1$ form factor. Figure 8 shows the calculated transverse form factor (solid curve) and (e,e′) data for the transition to the 3.563-MeV state.

The second calculation employed a spin transition density obtained from the empirical shell-model wave functions of Donnelly and Walecka.[13] These wave functions are almost identical to the pure LS-coupling p-shell wave functions. Using p-shell harmonic oscillator radial wave functions for the valence nucleons, Donnelly and Walecka

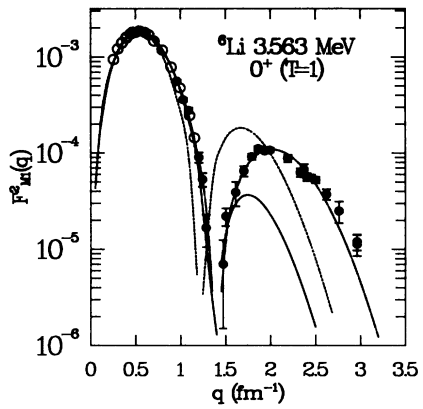

FIG. 8. $F_T^2(q)$ for the 0^+, $T=1$, 3.563-MeV state of ^{6}Li. The calculations used a microscopic transition density derived from Cohen-Kurath intermediate-coupling p-shell wave functions (solid curve) with $\alpha=0.518$ fm^{-1} and a renormalization constant of 0.97, a microscopic transition density derived from the empirical shell-model wave functions of Donnelly and Walecka (dashed curve) with $\alpha=0.493$ fm^{-1} and a renormalization constant of 0.96, and a phenomenological transition density based on the work of Bergstrom *et al.* (dash-dot curve). The data are from Refs. 14 (solid circles) and 37 (open circles).

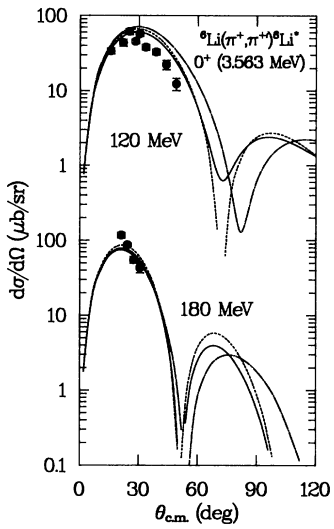

FIG. 9. Angular distributions for π^+ inelastic scattering to the 0^+, $T=1$, 3.563-MeV state of ^{6}Li for $T_\pi=120$ and 180 MeV. The calculations used a microscopic transition density derived from Cohen-Kurath intermediate-coupling p-shell wave functions (solid curve) with $\alpha=0.518$ fm^{-1} and a renormalization constant of 0.97, a microscopic transition density derived from the empirical shell-model wave functions of Donnelly and Walecka (dashed curve) with $\alpha=0.493$ fm^{-1} and a renormalization constant of 0.96, and a phenomenological transition density based on the work of Bergstrom *et al.* (dash-dot curve).

determined the one-body density matrix elements from normalization conditions and from fits to the ground state magnetic dipole and electric quadrupole moments and the $M1$ form factors for electron elastic and inelastic scattering for $q<1.01$ fm^{-1}.[13] A harmonic oscillator parameter[13] $\alpha=0.493$ fm^{-1} and a renormalization constant of 0.96 were used in our calculations. The resultant inelastic $M1$ form factor (dashed curve) is compared to the (e,e') data in Fig. 8.

The third analysis used a phenomenological spin transition density based on the work of Bergstrom *et al.*[14] This transition density was derived in the same manner as the transition density of Donnelly and Walecka except that we fitted the (e,e') data of Refs. 14 and 37, which extend to $q=2.96$ fm^{-1}, and assumed a polynomial form for the p-shell radial transition density. The wave functions for the ^{6}Li ground state and 3.563-MeV state were taken to be described by the SASK-A amplitudes of Bergstrom *et al.*[14] The radial transition density has a phenomenological form

$$R^2(r)=e^{-r^2/b^2}(a_2r^2+a_4r^4+a_6r^6)\ , \tag{3}$$

with $b=2.02$ fm, $a_2=6.625\times10^{-2}$ fm^{-5}, $a_4=-5.036\times10^{-3}$ fm^{-7}, and $a_6=1.967\times10^{-4}$ fm^{-9}, yielding a reduced χ^2 of 1.32 from a fit to the inelastic $M1$ form factor, which is presented in Fig. 8 (dash-dot curve).

The π^+ data and DWIA calculations at $T_\pi=120$ and 180 MeV for the spin-flip transition to the 3.563-MeV state are shown in Fig. 9. At 120 MeV the three spin transition densities give equivalent shapes for the angular distributions in the range of our data, $15.7°\le\theta_{c.m.}\le48.9°$. All calculations predict the correct location for the first maximum of $\theta_{c.m.}=28°$. However, the Cohen-Kurath intermediate-coupling (solid curve), Donnelly and Walecka (dashed curve), and phenomenological (dash-dot curve) calculations overestimate the magnitude of the first maximum by 18%, 29%, and 38%, respectively. The three spin transition densities yield similar results for the shape of the 180-MeV angular distribution through the first minimum but differ through the second maximum and minimum. Each calculation underestimates the magnitude of the first maximum by at least 26%.

The π^+ 3.563-MeV excitation function data and DWIA analyses are presented in Fig. 10. The momentum transfer for the excitation function was determined to be $q\simeq109$ MeV/c from the first maximum of the 120-MeV angular distribution. All other data points for the various energies are within +4% of this q. None of the spin transition densities predict the measured shape and magnitude of the 3.563-MeV excitation function. The Cohen-Kurath intermediate-coupling, Donnelly and Walecka, and phenomenological calculations disagree with the data by at least $\simeq$20% at both the low and high incident pion energies.

IV. DISCUSSION AND RESULTS

The disagreement between theory and data for the 120- and 180-MeV angular distributions and excitation function for the unnatural-parity transition to the 3.563-MeV state is difficult to understand, as is the disagreement observed for the unnatural-parity transition to the 15.11-MeV state of ^{12}C. For comparison, the 12.71- and 15.11-MeV excitation functions along with DWIA calculations as described in Ref. 10 are shown in Fig. 11. As noted in

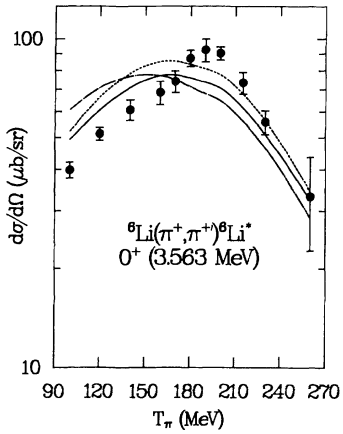

FIG. 10. Excitation function at a constant $q \simeq 109$ MeV/c for π^+ inelastic scattering to the 0^+, $T=1$, 3.563-MeV state of ^{6}Li. The calculations used a microscopic transition density derived from Cohen-Kurath intermediate-coupling p-shell wave functions (solid curve) with $\alpha=0.518$ fm^{-1} and a renormalization constant of 0.97, a microscopic transition density derived from the empirical shell-model wave functions of Donnelly and Walecka (dashed curve) with $\alpha=0.493$ fm^{-1} and a renormalization constant of 0.96, and a phenomenological transition density based on the work of Bergstrom *et al.* (dash-dot curve).

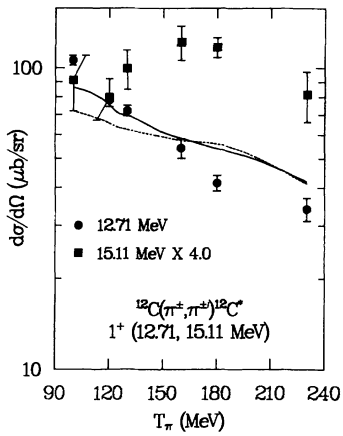

FIG. 11. Excitation functions (averaged π^+ and π^- cross sections to remove isospin mixing) at a constant $q=124$ MeV/c for pion inelastic scattering to the 1^+, $T=0$, 12.71-MeV (circles) and 1^+, $T=1$, 15.11-MeV (squares) states of ^{12}C. The calculations used microscopic transition densities derived from Cohen-Kurath p-shell wave functions. The solid curve is for the 12.71-MeV state. The dashed curve is for the 15.11-MeV state and has been multiplied by four (see Ref. 10).

the Introduction, a simple DWIA description of pion-nucleus inelastic scattering, which uses a single component of the pion-nucleon interaction and a single transition density, has been successful in describing unnatural-parity transitions in many nuclei. Using the zero-range spin-orbit operator and a spin transition density derived from Cohen-Kurath p-shell wave functions, Morris *et al.*[10] adequately reproduced the experimental 12.71-MeV excitation function. Furthermore, Cottingame *et al.*[12] adequately describe the 12.71-MeV angular distributions for $T_\pi=100$–260 MeV. Even though there is an energy-dependent enhancement near $T_\pi=180$ MeV in the 15.11-MeV excitation function,[10] the low-energy ($T_\pi=100$ and 116 MeV) angular distributions for this state are reproduced by simple DWIA calculations.[12] Using the same zero-range spin-orbit operator and three different spin transition densities, we cannot adequately describe either the 120- and 180-MeV angular distributions or the excitation function of the transition to the 3.563-MeV state. However, we are able to reproduce the angular distributions and constant-q differential cross sections at energies from $T_\pi=100$ to 260 MeV for the natural-parity transitions to the 2.185- and 4.25-MeV levels of ^{6}Li using only the central component of the pion-nucleon interaction and transition densities derived from Cohen-Kurath p-shell wave functions. The configuration-space, zero-range form of the spin-dependent component of the pion-nucleon interaction of Carr *et al.*[9] is most likely not in error. Furthermore, the transition densities we used for the transition to the 3.563-MeV level yield inelastic $M1$ form factors which agree with the (e,e') data for $q \lesssim 1.4$ fm^{-1} (see Fig. 8), which is a range of q that adequately covers the $q \simeq 0.55$ fm^{-1} at which the excitation function was measured. However, this does not eliminate uncertainties in the spin transition densities since the electron-scattering inelastic $M1$ form factor depends upon both the orbital and spin transition densities. Petrovich *et al.*[32] noted that the monopole spin transition densities derived from both the pure LS- and Cohen-Kurath intermediate-coupling p-shell wave functions produced Gamow-Teller matrix elements 17.9% and 8.4% larger than the experimental values. Also, Petrovich *et al.*[32] did not obtain agreement between theory and their ^{6}Li(p,p')^{6}Li*(3.563 MeV) data at $E_p \simeq 25$ MeV, with the theory failing to reproduce either the shape or magnitude of the angular distribution. This disagreement, however, was not attributed to uncertainties in the spin transition density, but Petrovich *et al.* suggested that other reaction processes in addition to the direct, one-step reaction process were contributing to the transition. Furthermore, Cammarata and Donnelly,[38] in their study of the reaction ^{6}Li(γ,π^+)^{6}He near threshold, conclude that the ratio of the orbital and spin transition densities derived from the Donnelly and Walecka wave functions[13] is probably correct. Thus, as is the case for the 15.11-MeV state of ^{12}C (Ref. 10), the disagreement between our simple DWIA analyses and the 3.563-MeV angular distributions and excitation function is difficult to explain as due to uncertainties in the spin transition density or the spin-dependent piece of the pion-nucleus inelastic interaction.

Since simple DWIA calculations using a well-tested spin-dependent component of the pion-nucleus inelastic interaction and spin transition densities obtained from fits to (e,e') data fail to reproduce both the shapes and magnitudes of the 3.563- and 15.11-MeV excitation functions, we suggest that the same mechanism may be responsible for the observed energy-dependent anomalous shapes in both ^{6}Li and ^{12}C. A possible mechanism is the direct ex-

citation of Δ-h components of the excited state wave functions, as proposed in Ref. 10. Within this Δ-h model interpretation, we can estimate the amount of Δ-h admixture in the 3.563-MeV wave function. Using the peak of the 3.563-MeV excitation function ($T_\pi = 190$ MeV), the DWIA calculation which used the phenomenological spin transition density, and the procedure of Refs. 10 and 39, we estimate a mixing matrix element of $3 \leq \kappa \leq 37$ MeV. This range of values of κ is similar to that estimated for the 15.11-MeV state of ^{12}C ($7.4 \leq \kappa \leq 27.3$ MeV).[39] However, if the direct excitation of Δ-h components is applicable to both transitions, comparison of the two excitation functions and DWIA calculations (see Figs. 10 and 11) indicate that the resonant Δ-h scattering amplitude may interfere differently with the p-h scattering amplitude for the two transitions.

V. CONCLUSIONS

Describing pion-nucleus inelastic scattering with the Born approximation and DWIA, we obtain predictions which agree with the π^+-inelastic-scattering measurements for the 3^+, 2.185-MeV and 2^+, 4.25-MeV states of ^{6}Li. Our predictions fail to reproduce both the 120- and 180-MeV angular distributions and the excitation function for the unnatural-parity transition to the 3.563-MeV state. The measured excitation function exhibits an anomalous energy-dependent shape similar to that observed for the 1^+, 15.11-MeV state of ^{12}C. Similar mechanisms may be responsible for the anomalous excitation functions for these isovector transitions. If this mechanism is the direct excitation of Δ-h components in the final state wave functions, the peak of the 3.563-MeV excitation function is reproduced with an estimated mixing matrix element of $3 \leq \kappa \leq 37$ MeV, a range of values consistent with the estimated mixing matrix element of $7.4 \leq \kappa \leq 27.3$ MeV (Ref. 39) for the 15.11-MeV excitation function.

ACKNOWLEDGMENTS

The authors thank F. Petrovich and J. A. Carr for their assistance in incorporation of the spin-dependent component of the pion-nucleon interaction into the computer code UTDWPI. This work was supported in part by the U. S. Department of Energy, the Robert A. Welch Foundation, and the Natural Sciences and Engineering Research Council of Canada.

*Present address: Kirtland Air Force Base, Albuquerque, NM 87117.
†Present address: Intel, Rio Rancho, NM 87124
‡Present address: University of New Mexico, Albuquerque, NM 87131.
§Present address: Los Alamos National Laboratory, Los Alamos, NM 87545.
**Present address: International Center for Theoretical Physics, Miramare, Trieste, Italy.

[1]T.-S. H. Lee and D. Kurath, Phys. Rev. C **21**, 293 (1980).
[2]T.-S. H. Lee and R. D. Lawson, Phys. Rev. C **21**, 679 (1980).
[3]Christopher L. Morris, Kenneth G. Boyer, C. Fred Moore, Carol J. Harvey, K. J. Kallianpur, Ingrid B. Moore, Peter A. Seidl, Susan J. Seestrom-Morris, D. B. Holtkamp, Steven J. Greene, and William B. Cottingame, Phys. Rev. C **24**, 231 (1981).
[4]Kenneth G. Boyer, William B. Cottingame, L. E. Smith, Steven J. Greene, C. Fred Moore, J. S. McCarthy, R. C. Minehart, J. F. Davis, G. R. Burleson, G. Blanpied, Chuck A. Goulding, Henry A. Thiessen, and Christopher L. Morris, Phys. Rev. C **24**, 598 (1981).
[5]W. B. Cottingame, K. Allbright, S. Greene, C. Harvey, D. B. Holtkamp, R. J. Joseph, I. B. Moore, C. F. Moore, J. Piffaretti, C. L. Morris, N. King, R. L. Boudrie, J. Kraushaar, R. J. Peterson, B. Ristinen, and G. R. Smith, Bull. Am. Phys. Soc. **24**, 821 (1979).
[6]S. J. Seestrom-Morris, D. Dehnhard, D. B. Holtkamp, and C. L. Morris, Phys. Rev. Lett. **46**, 1447 (1981).
[7]E. R. Siciliano and G. E. Walker, Phys. Rev. C **23**, 2661 (1981).
[8]M. K. Gupta and G. E. Walker, Nucl. Phys. **A256**, 444 (1976).
[9]J. A. Carr, F. Petrovich, D. Halderson, D. B. Holtkamp, and W. B. Cottingame, Phys. Rev. C **27**, 1636 (1983).
[10]C. L. Morris, W. B. Cottingame, S. J. Greene, C. J. Harvey, C. Fred Moore, D. B. Holtkamp, S. J. Seestrom-Morris, and H. T. Fortune, Phys. Lett. **108B**, 172 (1982).
[11]S. Cohen and D. Kurath, Nucl. Phys. **73**, 1 (1965), as quoted in T.-S. H. Lee and D. Kurath, Phys. Rev. C **21**, 293 (1980).
[12]W. B. Cottingame, K. G. Boyer, W. J. Braithwaite, S. J. Greene, C. J. Harvey, R. J. Joseph, D. B. Holtkamp, C. Fred Moore, J. J. Kraushaar, R. J. Peterson, R. A. Ristinen, R. L. Boudrie, N. S. P. King, C. L. Morris, J. Piffaretti, and H. A. Thiessen, submitted to Phys. Rev. C.
[13]T. W. Donnelly and J. D. Walecka, Phys. Lett. **44B**, 330 (1973).
[14]J. C. Bergstrom, U. Deutschmann, and R. Neuhausen, Nucl. Phys. **A327**, 439 (1979).
[15]H. A. Thiessen and S. Sobottka, Los Alamos Scientific Laboratory Report No. LA-4534 MS, 1970.
[16]D. F. Geesaman, D. Kurath, G. C. Morrison, C. Olmer, B. Zeidman, R. E. Anderson, R. L. Boudrie, H. A. Thiessen, G. S. Blanpied, G. R. Burleson, R. E. Segel, and L. W. Swenson, Phys. Rev. C **27**, 1134 (1983).
[17]Lester Eugene Smith, computer program LOAF (unpublished).
[18]F. Ajzenberg-Selove, Nucl. Phys. **A413**, 28 (1984).
[19]F. Eigenbrod, Z. Phys. **228**, 337 (1969).
[20]Th. Delbar, Gh. Grégoire, and G. Paić, Phys. Rev. C **27**, 1887 (1983).
[21]G. R. Burleson and J. F. Amann, computer program CROSS (unpublished).
[22]C. Rowe, M. Salomon, and R. H. Landau, Phys. Rev. C **18**, 584 (1978).
[23]W. B. Cottingame and D. B. Holtkamp, Phys. Rev. Lett. **45**, 1828 (1980).
[24]R. A. Eisenstein and G. A. Miller, Comput. Phys. Commun. **8**, 130 (1974).
[25]L. S. Kisslinger, Phys. Rev. **98**, 761 (1955).
[26]G. C. Li, I. Sick, R. R. Whitney, and M. R. Yearian, Nucl. Phys. **A162**, 583 (1971).

[27]Janos A. Zichy, Ph.D. dissertation, Eidgenôssische Technische Hochschule Report No. ETH-6612, 1980.
[28]J. A. Carr, F. Petrovich, D. Halderson, and J. Kelly (unpublished).
[29]K. G. Boyer, W. B. Cottingame, and D. B. Holtkamp, distorted wave code UTDWPI (unpublished), adapted from the code DWPI by R. A. Eisenstein and G. A. Miller, Comput. Phys. Commun. **11**, 95 (1976).
[30]R. Neuhausen and R. M. Hutcheon, Nucl. Phys. **A164**, 497 (1971).
[31]F. Petrovich and W. G. Love, Nucl. Phys. **A354**, 499c (1981).
[32]F. Petrovich, R. H. Howell, C. H. Poppe, S. M. Austin, and G. M. Crawley, Nucl. Phys. **A383**, 355 (1982).
[33]J. A. Carr, private communication.
[34]J. C. Bergstrom and E. L. Tomusiak, Nucl. Phys. **A262**, 196 (1976).
[35]M. Bernheim and G. R. Bishop, Phys. Lett. **5**, 270 (1963).
[36]J. C. Bergstrom, S. B. Kowalski, and R. Neuhausen, Phys. Rev. C **25**, 1156 (1982).
[37]J. C. Bergstrom, I. P. Auer, and R. S. Hicks, Nucl. Phys. **A251**, 401 (1975).
[38]J. B. Cammarata and T. W. Donnelly, Nucl. Phys. **A267**, 365 (1976).
[39]C. L. Morris, in *Spin Excitations in Nuclei,* edited by Petrovich, Brown, Garvey, Goodman, Lindgren, and Love (Plenum, New York, 1984), p. 161ff.